Journal of
Applied Remote Sensing

RemoteSensing.SPIEDigitalLibrary.org

Vegetation role in controlling the ecoenvironmental conditions for sustainable urban environments: a comparison of Beijing and Islamabad

Shahid Naeem
Chunxiang Cao
Mirza Muhammad Waqar
Chen Wei
Bipin Kumar Acharya

SPIE.

Shahid Naeem, Chunxiang Cao, Mirza Muhammad Waqar, Chen Wei, Bipin Kumar Acharya, "Vegetation role in controlling the ecoenvironmental conditions for sustainable urban environments: a comparison of Beijing and Islamabad," *J. Appl. Remote Sens.* **12**(1), 016013 (2018), doi: 10.1117/1.JRS.12.016013.

Vegetation role in controlling the ecoenvironmental conditions for sustainable urban environments: a comparison of Beijing and Islamabad

Shahid Naeem,[a,b] Chunxiang Cao,[a,b,*] Mirza Muhammad Waqar,[c] Chen Wei,[a,b] and Bipin Kumar Acharya[a,b]

[a]University of Chinese Academy of Sciences, Beijing, China
[b]Institute of Remote Sensing and Digital Earth, State Key Laboratory, Division of Environmental Health, Beijing, China
[c]Chiba University, Center for Environmental Remote Sensing, Japan

Abstract. The rapid increase in urbanization due to population growth leads to the degradation of vegetation in major cities. This study investigated the spatial patterns of the ecoenvironmental conditions of inhabitants of two distinct Asian capital cities, Beijing of China and Islamabad of Pakistan, by utilizing Earth observation data products. The significance of urban vegetation for the cooling effect was studied in local climate zones, i.e., urban, suburban, and rural areas within 1-km^2 quantiles. Landsat-8 (OLI) and Gaofen-1 satellite imagery were used to assess vegetation cover and land surface temperature, while population datasets were used to evaluate environmental impact. Comparatively, a higher cooling effect of vegetation presence was observed in rural and suburban zones of Beijing as compared to Islamabad, while the urban zone of Islamabad was found comparatively cooler than Beijing's urban zone. The urban thermal field variance index calculated from satellite imagery was ranked into the ecological evaluation index. The worst ecoenvironmental conditions were found in urban zones of both cities where the fraction of vegetation is very low. Meanwhile, this condition is more serious in Beijing, as more than 90% of the total population is living under the worst ecoenvironment conditions, while only 7% of the population is enjoying comfortable conditions. Ecoenvironmental conditions of Islamabad are comparatively better than Beijing where ~61% of the total population live under the worst ecoenvironmental conditions, and ~24% are living under good conditions. Thus, Islamabad at this early growth stage can learn from Beijing's ecoenvironmental conditions to improve the quality of living by controlling the associated factors in the future. [DOI: 10.1117/1.JRS.12.016013]

Keywords: population growth; earth observation data; quality of living; vegetation degradation; ecoenvironmental conditions.

Paper 170671 received Jul. 28, 2017; accepted for publication Dec. 8, 2017; published online Jan. 18, 2018.

1 Introduction

Intense urbanization due to population growth and the increase in anthropogenic activities has transformed the world's landscapes and urban ecosystem rather actively in the last few decades. Increasing trends in industrialization and urbanization are the extreme factors that are influencing the land surface transformation.[1] Urbanization is the major activity that is contributing dynamically to change the land use/land cover (LULC),[2–4] modifying the energy balance and making the city areas warmer than the rural areas. Modern transportation and industries are adding to the greenhouse gases in the atmosphere. The activity of the replacement of the natural vegetation area into buildings at a fast rate is threatening. This is because of the usage of low

*Address all correspondence to: ChunXiang Cao, E-mail: caocx@radi.ac.cn

albedo materials, leading to higher heat absorption in urban centers and causing the significantly higher surface temperature of the urban boundary than its surroundings. These hot areas are just like an island in a sea of relatively cooler areas and termed as the urban heat islands (UHI).[5] UHI not only cause a change in biodiversity but are also responsible for human discomfort by spreading different diseases causing disease and mortality.[6] UHIs increase the energy consumption to generate cooling, hence emitting CO_2.[7]

There are many reasons for the increase in land surface temperature (LST) of urban areas, but three of them are contributing more actively. The first reason is the extensive use of water-resistant construction materials, which do not allow evapotranspiration to occur rather actively. The second one is impervious surfaces absorb more incoming heat from the Sun than natural vegetation.[8] The third one is the vegetative areas are being transformed into urban and industrial land. Many other parameters are making a significant impact on the rise in temperature, for example: the change in latitudes, wind speed, elevation, topography, and size of the city.[7] Almost all of the cities in the world experience higher LST in their urban periphery than their surroundings.

Earth observation (EO)-supported data have encouraged large-scale research on the UHI across the continents for both large- and small-sized cities of the world.[9] It has been proven to be a powerful source for the studies of temporal dynamics and spatial patterns of the thermal landscape and the surface energy budget for urban areas.[10] The EO-data acquired through the remote sensing process provide not only the inclusive information of LULC but also the LST observation with a uniform sampling.[11] Many sensors, such as Landsat (TM, ETM+, and OLI), moderate resolution imaging spectroradiometer (MODIS), advanced spaceborne, thermal emission and refraction, advanced very high resolution radiometer, and some others, are being used to extract the LST.[9] UHI studies are normally carried out by extracting LST from the thermal infrared (TIR) band of satellite-derived data. Therefore, studies have proven remote sensing data to be a valuable and powerful source for these kinds of ecological research works at various spectral, spatial, and temporal scales.

Most of the remote sensing research methodologies on UHI focused on the LULC and associated surface temperature changes. Previous studies have shown a strong relationship between LST and LULC.[12] The formation of UHI was explored from the LULC change and the surface temperature calculated from remotely sensed data. Urbanization is responsible for the changes in LULC because impervious surfaces such as asphalt, metal, and concrete are replacing the natural vegetation areas.[7,13] To study the effect of the change in LULC on thermal environments, Shi and Ding[14] used the Landsat data of Beijing and related land use/cover with LST. Similarly, Alavipanah et al.[15] studied the vegetation role to mitigate the urban LST in Munich, Germany, and concluded that the urban vegetation plays an important role in the cooling of impervious surfaces, and the optimum green spaces are required to lower the surface temperature. They have shown a good negative relation between LST and the proportion of the urban vegetation. This trend was nonlinear and showed cooler LST in the areas where the proportion of the urban vegetation present was between 70% and 80%. Ogashawara and Bastos[16] used a quantitative approach to analyze the relation among land cover, surface temperature, and several model indices, such as the normalized difference vegetation index (NDVI), the normalized difference built-up index (NDBI), and the normalized difference water index (NDWI). Their results show a positive correlation of bare soil and urban areas with surface temperature, whereas the correlation of vegetation and water bodies with surface temperature was found to be negative. On the other hand, the correlations of NDWI and NDVI with LST were low, but the corresponding correlation between NDBI and surface temperature was moderate. Xiong et al.[17] studied the impacts of change in urban areas on the thermal environment. The study concluded that spatiotemporal variations of the urban thermal environment can be attributed to the rapid increase in urbanization of Guangzhou. The main reasons for the increase in the amounts of waste heat are vegetation degradation coverage, increase in built-up areas, and intensity of anthropogenic activities. Kuang et al.[18] analyzed the difference in LST for different LULC classes by using *in situ* observations and concluded that impervious surfaces are relatively warmer than green areas. Li et al.[19] calculated LST and NDVI to understand the impact of LULC change on the Shanghai landscape. Similarly, Zhou et al.[20] applied spatial analysis on multilevels to detect the change in urban vegetation at the individual tree scale. Ahmed et al.[21] simulated the LULC changes to assess

their impacts on LST in Dhaka. Jiang et al.[22] conducted a study in the United States to assess the impacts of LULC change associated with surface temperature and surface moisture. The study tested both NDWI and soil moisture as measures of the urban area's surface moisture and concluded that NDWI was found to be more sensitive than soil moisture for the land cover changes.

The surface temperature patterns of urban, suburban, and rural vegetation were studied for Islamabad and Beijing. This *in situ* zonation was defined according to the local climate zones (LCZ) concept of Stewart and Oke. The authors described that LCZ are the regions of uniform surface cover, material, structure, and human activity. The horizontal scale can vary from a few hundreds of meters to several kilometers having similar thermal microclimates.[23] As EO studies of urban vegetation have shown cooler surface temperatures in vegetated areas than impervious surfaces of cities,[24] thus urban green vegetation can play a significant role in controlling the ecoenvironmental conditions and the mitigation of climate change to raise the quality of living at the local, as well as the global level. Quality of living can not only be improved by simultaneous cooling mechanisms (shading, evapotranspiration, and increasing albedo) but also by lowering the summertime energy demands to cool indoor climates can also play a significant role in this case, by decreasing CO_2 emissions. Urban greening is also a proposed approach for the mitigation of human health consequences of the increase in temperatures because of climate change scenarios.[24] Urban vegetation, however, not only mitigates climate change but also works as a supporting element in the safety of urban life, social cohesion, and ecological values.[25]

The study was conducted to evaluate the environmental conditions of two capital cities based on EO-supported ecoenvironmental indices. Beijing is heavily urbanized city and expanding rapidly as compared to Islamabad. A lot of research work on environmental issues of Beijing has already been done but Islamabad is a poorly studied area and no scientific research has been done on environmental problems so far. Although, the present environmental situation of Islamabad is not as critical as in the case of Beijing, being a capital city of the country it is expected to expand rapidly in the near future and can face the same environmental problems. Therefore, this study is carried out to highlight the cooling effect of surrounding vegetation in Islamabad in comparison to Beijing for climate smart development.

The primary objective of the study is to compare the cooling effect of vegetation in LCZ. Both capital cities were categorized into three basic LCZ, and in each zone, the cooling effect of vegetation was analyzed and compared by calculating the vegetation fractions within 1×1 km^2 quantiles. The ecological evaluation index was applied to compute the spatial distribution of the intensity of the UHI phenomenon and ecoenvironmental conditions. This index has already been used in some researches to evaluate the spatial patterns of UHI intensity, but in the present study, it was used to indicate the inhabitants under poor, normal and good eco-environmental conditions. Population distribution was used to evaluate environmental impact by indicating the inhabitants under poor, normal, and good ecoenvironmental conditions. The ecological evaluation index has rarely been used for this purpose in previous researches. The two cities were selected for the purpose of cross-learning, by which Islamabad being at an early growth stage can learn from Beijing at a later growth stage. Along with the cross-learning, the results of the study highlighting areas under poor ecoenvironmental conditions will facilitate urban planners for designing appropriate recovery and management plans.

2 Materials and Methods

2.1 *Study Area*

The study was composed of two capital cities of China and Pakistan (Beijing and Islamabad) (Fig. 1). Beijing is the capital of China. It extends from 39°26′N–41°03′N in latitude and 115°25′E–117°30′E in longitude. The latitudinal difference is ~1°37′, and the longitudinal difference is 2°05′. Its elevation for the urban region varies from 50 to 200 m, whereas for hilly areas, it varies from 200 to 1700 m. The total area of Beijing is 16,410 km^2, and it is covered by 14 districts with two counties[26] (Fig. 1). The climate of the city is subhumid warm temperate monsoon with four distinct seasons. Normally, Beijing's people have to face hot and humid summer and cold

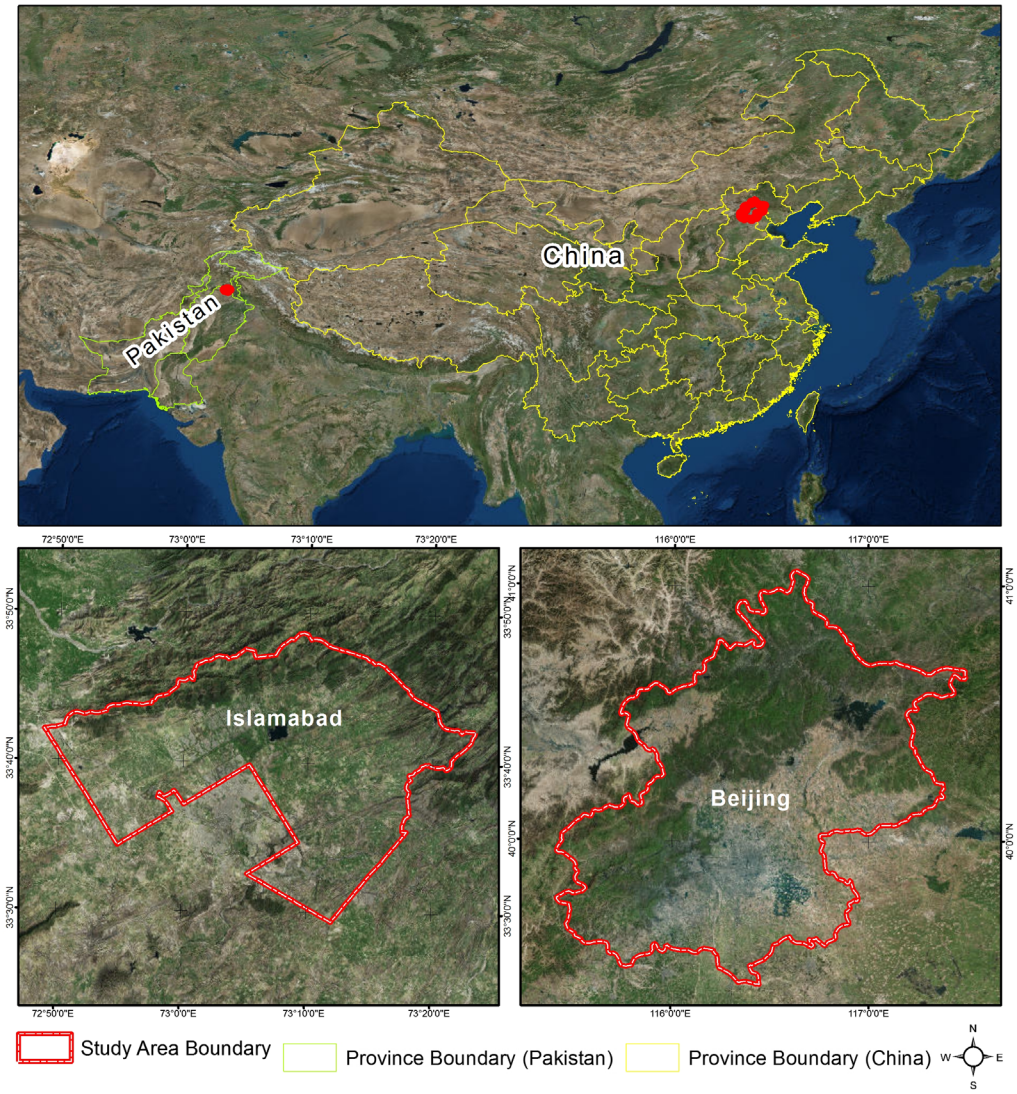

Fig. 1 Location map of the study area.

and windy winter seasons. Beijing is experiencing a rapid urbanization process. In 1989, its permanent population was reported to be 10.75 million, but in 2010, this figure reached up to 19.62 million. On the other hand, gross domestic product has increased by ~30 times, from 45.6 to 1411.3 billion from 1989 to 2010.[26] Due to rapid urbanization in Beijing, currently there are many environmental problems, such as UHI, air pollution, smog, sand, and dust storms. These factors are the major by-products of rapid population growth, leaving a negative effect on the comfort and quality of urban living.[27] Environmental problems in Beijing, especially UHI and air pollution, have drawn the attention of international agencies. Zhang et al.[28] reported that the average UHI was ~4°C to 6°C while using a suburban area in the northwestern region as a rural baseline and 8°C to 10°C while using the outer suburban area in the same region. The timing of the fall foliage vacationing season has even been delayed due to warmer temperatures.[29] If this trend, the diversified and rapid development of urban society and the economy, continues, the urban extent of Beijing will probably expand, and the UHI effect will be more severe.[30]

Islamabad is the capital of the Islamic Republic of Pakistan. The elevation of the city is about 500 to 600 m above sea level and located at 33°28′12″N–33°48′36″N latitude and 72°48′36″E–73°24′E longitude. Islamabad is flanked by the high Margalla Hills in its north (Fig. 1). The area of the city is about 906 km^2. The total population of the city is about

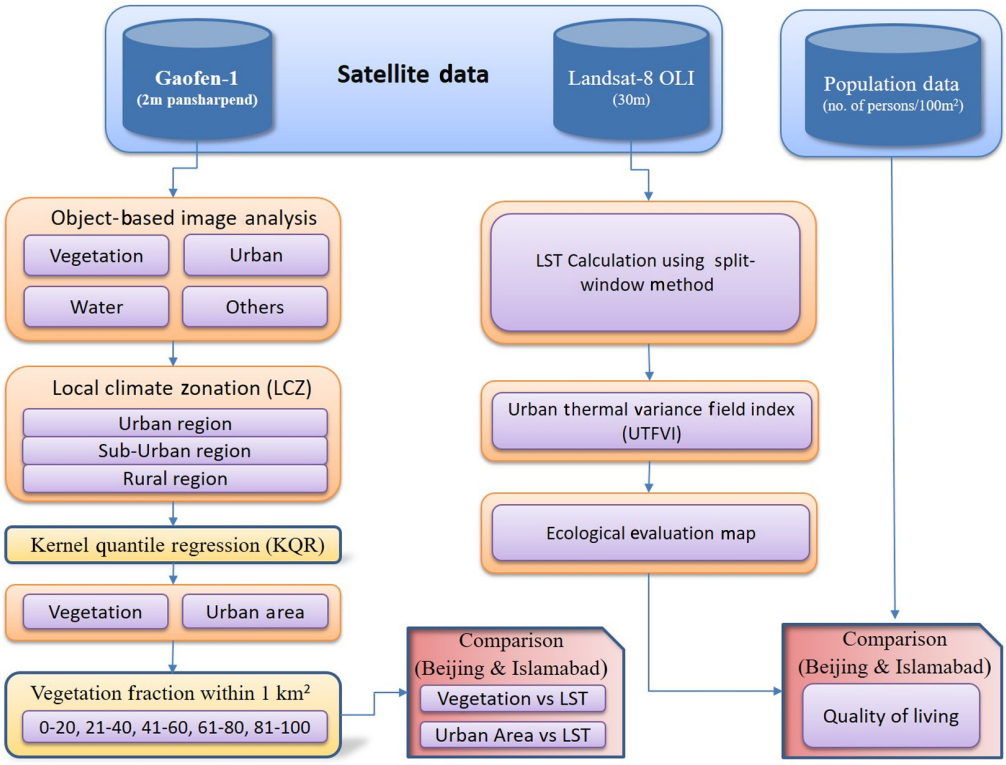

Fig. 2 Methodological framework.

1.2 million.[31] The climate of the city is humid and subtropical with four distinct seasons: summer, autumn, winter, and spring. Islamabad is divided into different zones, such as commercial, residential, industrial, and diplomatic. Marble factories, steel mills, flour mills, soap/chemical factories, oil units, pigments, paints, and pharmaceutical plants are some of the main industries in the city. The ever-increasing emissions from automobiles are also one of the main sources of air pollution in the city.[32]

2.2 *Methodological Approach*

The satellite datasets and methodological approach used for this study are summarized in the flow diagram in Fig. 2.

2.3 *Satellite Data Sources*

Two main satellite datasets: Gaofen-1 (GF-1) and Landsat-8 operational land imager (OLI) satellite imagery data were used in this study. The Landsat-8 (OLI) sensor contains three more bands than Landsat-7 (ETM+), deep blue shortwave infrared bands added for coastal ecosystem monitoring and cirrus detection, respectively, while two TIR bands provide improved radiometric resolution quantized as 12-bit range. TIR bands were used to calculate LST for this study (Table 1).

The first satellite of the series of optical high-resolution EO satellites mission of the China National Space Administration is Gaofen-1. GF-1 data (spatial resolution of 2 m) were used to develop the land cover and Landsat-8 data acquired by the OLI to calculate NDVI and NDBI. The thermal bands of a single image of Landsat-8 (OLI) were acquired for both cities. All satellite data were collected for the month of September 2015, to avoid phenological differences and incoming solar radiation. Before land cover classification and LST calculation, satellite images were preprocessed. Different preprocessing steps were applied including

Table 1 Satellite data specifications.

Satellite name	Spectral mode	Spatial resolution (m)
Gaofen-1	Multispectral	8×8
	Panchromatic	2×2
Landsat-8 (OLI)	Multispectral	30×30
	Panchromatic	15×15
	TIR	100×100

pan-sharpening, atmospheric corrections, and area of interest truncation. After land cover classification and LST calculation, thematic data were resampled to a 1-km^2 grid.

2.4 *Population Data*

Population data were downloaded from Ref. 33. These data provide the number of people residing within 100×100 m grid cell through an integrating survey, census, GIS, and remote sensing datasets. Different methods outlined by Deville et al., Alegana et al., and Stevens et al. were used for population counts and density mapping.[34–36] These-high resolution data are available from 2000 to 2020 along with metadata.[37] Population data from 2015 were used for this study.

2.5 *Land Surface Temperature Retrieval*

The methods of LST retrieval from the satellite thermal band can be further divided into three different categories: multichannel methods [split-window (SW) algorithm], single-channel methods, and multiangle methods.[38,39] In recent times, three different SW algorithms were used to calculate the LST from Landsat-8 TIR bands.[23,40] The single-channel algorithms for the retrieval of LST have been improved for Landsat-8 TIRS bands.[41] Wang et al. upgraded the monowindow algorithm for LST calculation from Landsat-8 thermal bands.[42,43] Comparatively, the monowindow algorithm requires only two atmospheric parameters, so it is a bit simpler method.[42] However, the SW method is considered to be more reliable and used more frequently in recent times; therefore, we applied the SW algorithm (a structured mathematical algorithm) for the calculation of LST. The SW method uses the brightness temperatures of two TIR bands (band 10 and band 11 of Landsat-8) by calculating the difference and mean in land surface emissivity (LSE) to estimate the LST of an area. The algorithm is given as

$$\begin{aligned} \mathrm{LST} = {} & \mathrm{TB}_{10} + C_1(\mathrm{TB}_{10} - \mathrm{TB}_{11}) + C_2(\mathrm{TB}_{10} - \mathrm{TB}_{11})^2 + C_o + (C_3 + C_4 W)(1 - \varepsilon) \\ & + (C_5 + C_6 W)\Delta\varepsilon, \end{aligned} \tag{1}$$

where LST refers to the LST (K); C_0, C_1, C_2, C_3, C_4, C_5, and C_6 are the values of the coefficient of the SW (Table 2);[44] TB_{10} and TB_{11} are the brightness temperatures of bands 10 and 11 in Kelvin; ε is the mean LSE of TIR bands; W is the water vapor content in the atmosphere; $\Delta\varepsilon$ is the LSE difference between TB_{10} and TB_{11}.

2.5.1 *Brightness temperature (T_B)*

T_B is a measure of microwave radiations that travels upward from the top portion of the Earth's atmosphere. The calibration process was done to convert digital number values to the brightness temperature (T_B). To calculate the TB of a particular area, the spectral radiance top of atmosphere (L_λ) is required. Using the following algorithm, T_B was calculated for both TIR bands

Table 2 SW coefficients.

Constant	Value
C_0	−0.268
C_1	1.3780
C_2	0.1830
C_3	54.300
C_4	−2.238
C_5	−129.2
C_6	16.400

$$T_B = \frac{K_2}{L_n\left[\left(\frac{K_1}{L_\lambda}\right)+1\right]}, \tag{2}$$

where K_1 and K_2 are the thermal conversion constants; L_λ is the spectral radiance of the top of the atmosphere.

The L_λ value was calculated by multiplying the rescaling factor (0.000342) with its corresponding TIR band and adding an additive rescaling factor (A_L).

$$L_\lambda = M_L Q_{\text{cal}} + A_L, \tag{3}$$

where L_λ is in watts/$(m_2 \times \text{srad} \times \mu\text{m})$; M_L is the multiplicative rescaling factor of a specific band; Q_{cal} is band 10 or 11; A_L is the additive rescaling factor of a specific band.

2.5.2 *Land surface emissivity*

LSE is very important to calculate the LST of a region. Therefore, the NDVI threshold method was adopted to estimate LSE. This method is explained as

$$\text{LSE} = \varepsilon_s(1 - \text{FVC}) + \varepsilon_v \text{FVC}, \tag{4}$$

where ε_v is the vegetative emissivity and ε_s is the and soil emissivity values of the corresponding bands, respectively (Table 3).[44]

The fractional vegetation cover (FVC) for an image was calculated from

$$\text{FVC} = \frac{\text{NDVI} - \text{NDVI}_s}{\text{NDVI}_v - \text{NDVI}_s}, \tag{5}$$

where NDVI_s and NDVI_v are the reclassified values of NDVI for soil and vegetation, respectively.

Table 3 Vegetation and soil emissivity values for Landsat-8 (OLI) band 10 and band 11.

Emissivity	Band 10	Band 11
ε_s	0.971	0.977
ε_v	0.987	0.989

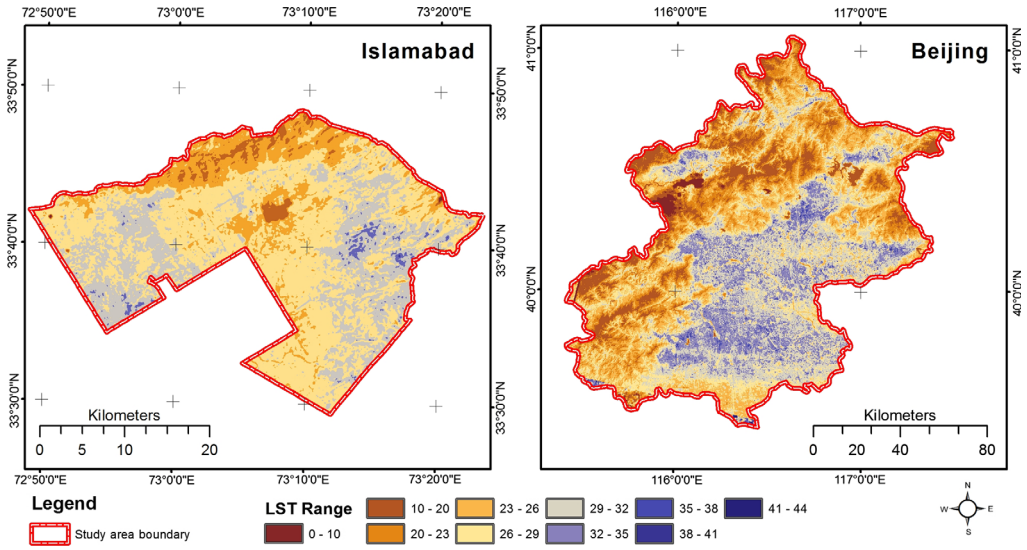

Fig. 3 LST map of Islamabad and Beijing.

2.5.3 *NDVI threshold*

The NDVI image was reclassified into vegetation and soil to determine the $NDVI_v$ and $NDVI_s$. These classified data were used to calculate FVC (Fig. 3). After calculating LSE for the bands of TIR, their mean and difference were extracted using

$$\varepsilon = \frac{(\varepsilon_{10} - \varepsilon_{11})}{2}, \tag{6}$$

$$\delta\varepsilon = \varepsilon_{10} - \varepsilon_{11}, \tag{7}$$

where ε is the mean LSE; $\delta\varepsilon$ is the difference in LSE of both TIR bands (10 and 11).

By putting these values in Eq. (1), finally LST was calculated in Kelvin, using the SW algorithm.

2.6 *Statistical Approach*

Considering the 2-m spatial resolution of GF-1 satellite data and the 100-m spatial resolution (resampled 30 m) of the thermal band of Landsat-8 imagery, it was important to define a single scale for statistical analysis. Therefore, a 1-km^2 grid was used to investigate the relationship of vegetation and built-up area with LST within each box.

The computation was executed for the LULC (especially vegetation) extracted from the GF-1 satellite data and LST calculated from Landsat-8 imagery. It was attained by considering the percentage of vegetation in each grid cell for urban, suburban, and rural areas. For this purpose, vegetation percentage and mean LST within each grid cell were calculated for all three regions of both study sites. The plotted values of LST and vegetation proportion within each grid cell for a specific region study area demonstrate the LST change in urban vegetation and built-up areas.

2.7 *Land Cover Classification and Local Climate Zonation*

We used Gaofen-1 (GF-1) satellite imagery for the land cover classification. GF-1 satellite data are high-resolution imagery with a spatial resolution of 2 m. To extract major land cover classes (especially vegetation and built-up area), the object-based image analysis (OBIA) approach[45] of Definiens Developer 7 was applied. Definiens Developer 7 is a commercial software that is specifically used for OBIA.[46] OBIA is a technique to analyze high-resolution satellite imagery,

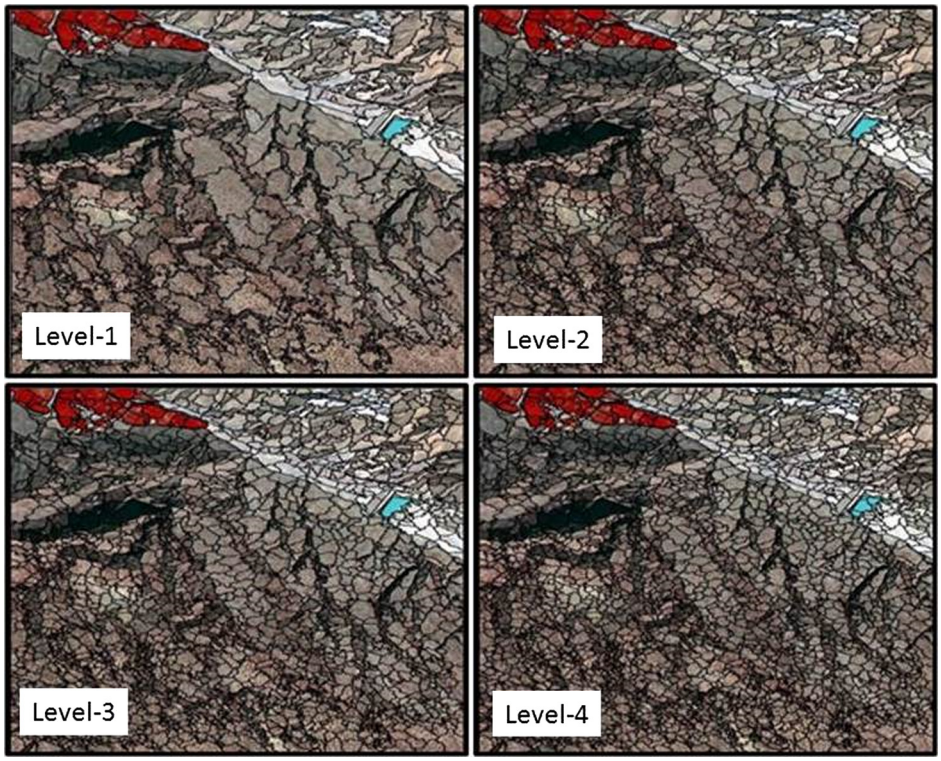

Fig. 4 Image segmentation.

and it has been used very frequently since the last decade. In the OBIA approach, image objects are used for analysis rather than individual pixels. The process of generating image objects is known as image segmentation. This process is usually handled by applying different homogeneity criteria such as layer weight, shape, and compactness.[45,47] The key advantages of OBIA are the saving of time and the reduction of noise.[47] In OBIA, image segments (shown in Fig. 4) are classified based on statistical spectral features of an image. This means image objects can be classified based on their texture, geometry, and shape.[48] To assign the class to image objects corresponding to real-world objects, two widely used OBIA methods can be used. These OBIA methods are: (1) rule-based methods: this method classifies image objects based on rules defined by the expert based on personal knowledge; (2) sample-based methods: this method assigns image objects to a class based on their similarity to samples, i.e., the distance of objects from samples in the feature space.[49,50]

To classify the satellite images, first of all, multiresolution segmentation was applied to develop the image objects. Multiresolution segmentation is a region growing method, and it is controlled by the scale parameter to determine the allowed heterogeneity to be created. This scale parameter is set up by the weighted heterogeneity of two other parameters, i.e., shape and color. Shape heterogeneity is set up as compactness and smoothness weightings. Different levels of the multiresolution segmentation approach were applied on the pan-sharpened images of Beijing

Table 4 Image segmentation parameters.

Hierarchy	Scale	Shape	Compactness
Level-1	30	0.1	0.9
Level-2	25	0.1	0.9
Level-3	20	0.1	0.9
Level-4	15	0.1	0.9

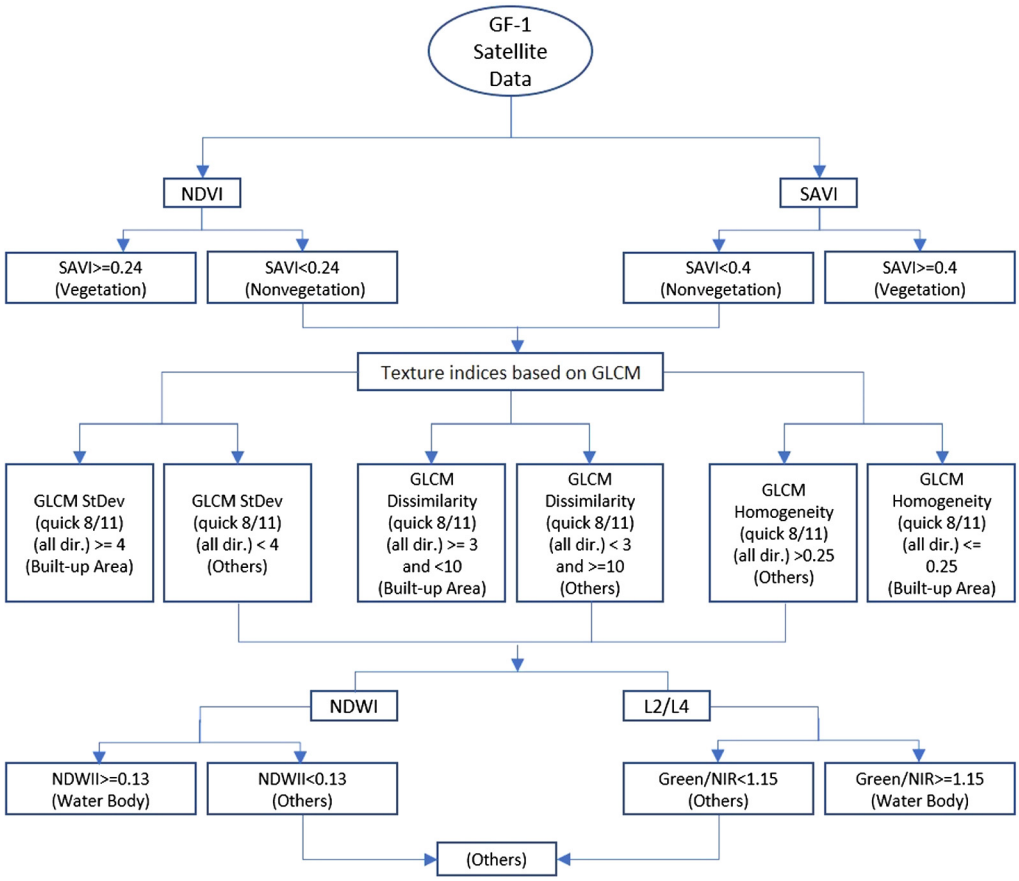

Fig. 5 Decision tree classifier for Image classification.

and Islamabad to generate image objects. Parameters used for this purpose are given in Table 4. The classification was done by defining different rulesets for different classes 5. Decision rule's criteria was slightly different for different satellite images, digital elevation model was also incorporated for a few images (Fig. 5).

Study sites were classified into four main classes, vegetation, built-up area, water, and others, but mainly focused on vegetation and built-up area classes to investigate the relationship of built-up area and the fraction of vegetation with LST. This is mainly to identify the role of the vegetation fraction in cooling and heating the land surface in both cities. After classification of both the Beijing and Islamabad areas, it was divided into three LCZ; urban, suburban, and rural zones, and it was based on the *in situ* situation. This zonation was defined according to the LCZ concept of Stewart and Oke.[51] The statistic and spatial patterns of vegetation cover and built-up areas are shown in Fig. 6. The accuracy assessment for Beijing and Islamabad is given in Tables 5–7.

For accuracy assessment, randomly selected sample points of homogeneous areas of all the classes were used as reference data. The reference points were selected from the centers of the classified segments and verified using high-resolution imagery of Google Earth. Those points were used as a reference data to verify the classified segments. The main focus was on vegetation and built-up area so most of the points were selected for these two classes.[52,53] The accuracies can be improved by applying support vector machine or random forest classifiers.[54–57]

To analyze the relationship of LST with the proportion of urban, suburban, and rural vegetation, quantiles were divided into five equal intervals, i.e., 0% to 20%, 21% to 40%, 41% to 60%, 61% to 80%, and 81% to 100%. This grouping was made to discriminate the fluctuations of the cooling effect due to the change in vegetation fraction.

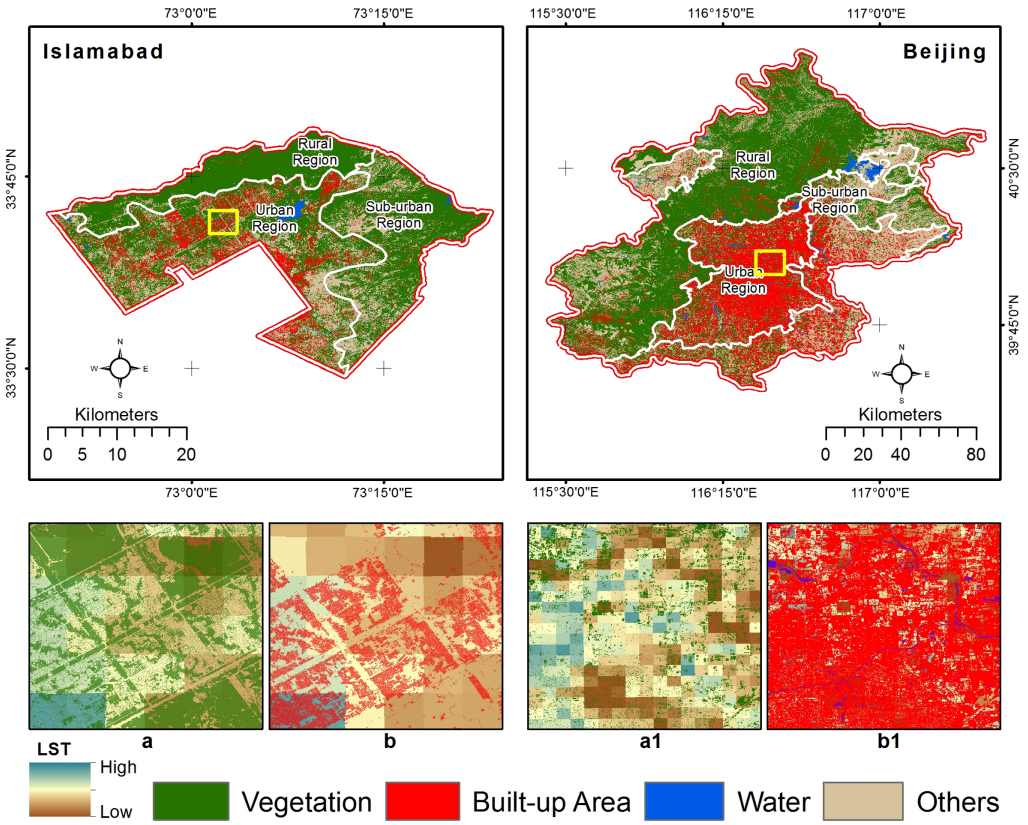

Fig. 6 Spatial patterns of vegetation and built-up area cover of Islamabad and Beijing, where a and a1 represent the vegetation patterns of Islamabad and Beijing, while b and b1 represent the built-up area pattern, respectively.

Table 5 Land cover statistics.

	% cover of Islamabad			% cover of Beijing		
Class name	Urban	Suburban	Rural	Urban	Suburban	Rural
Vegetation	48.59	69.76	93.30	21.83	20.96	67.58
Built-up area	19.58	2.80	1.17	64.26	29.60	5.93
Water	1.58	0.63	0.04	1.12	1.41	1.11
Others	30.25	26.81	5.49	12.79	48.03	25.38

Table 6 Accuracy assessment of the classified map of Islamabad.

Class name	No. of samples	Total sample area (ha)	User's accuracy (%)	Producer's accuracy (%)
Vegetation	85	78.2	89.43	88.24
Built-up area	42	31.5	85.81	82.65
Water	12	9.1	80.34	85.41
Others	28	20.9	79.01	77.34
Total	167	139.7		
Overall accuracy	83.6			

Table 7 Accuracy assessment of the classified map of Beijing.

Class name	No. of samples	Total sample area (ha)	User's accuracy (%)	Producer's accuracy (%)
Vegetation	147	139.6	90.13	91.39
Built-up area	110.1	31.5	84.81	85.51
Water	10	7.3	85.37	79.34
Others	61	44.7	75.72	81.46
Total	341	301.7		
Overall accuracy	84.01			

3 Results

3.1 *Relationship Between LST and Vegetation Fraction*

The descriptive statistical analysis of both cities revealed that the inner-city surface temperature is higher than the surface temperatures of suburban and rural regions. These temperature variations at the study sites are due to the capacity of the construction material to absorb heat and other thermal properties of core city area surfaces (Table 10). These factors elevate the temperature patterns of dense urban regions because impervious surfaces absorb more incoming solar radiation than the natural vegetation or bare areas. The results are shown in Figs. 7–9.

Figure 7 shows the rural regions' comparison of Beijing and Islamabad, with a higher mean surface temperature observed in the rural region of Islamabad than the same region for Beijing. It can be seen from Fig. 7 that the mean temperature is decreasing with the increase in vegetation fraction within quantiles of 1 km^2 in both cities. Beijing has more surface temperature variations than Islamabad, and in some areas, the lower limit of temperature is about 8°C, while the

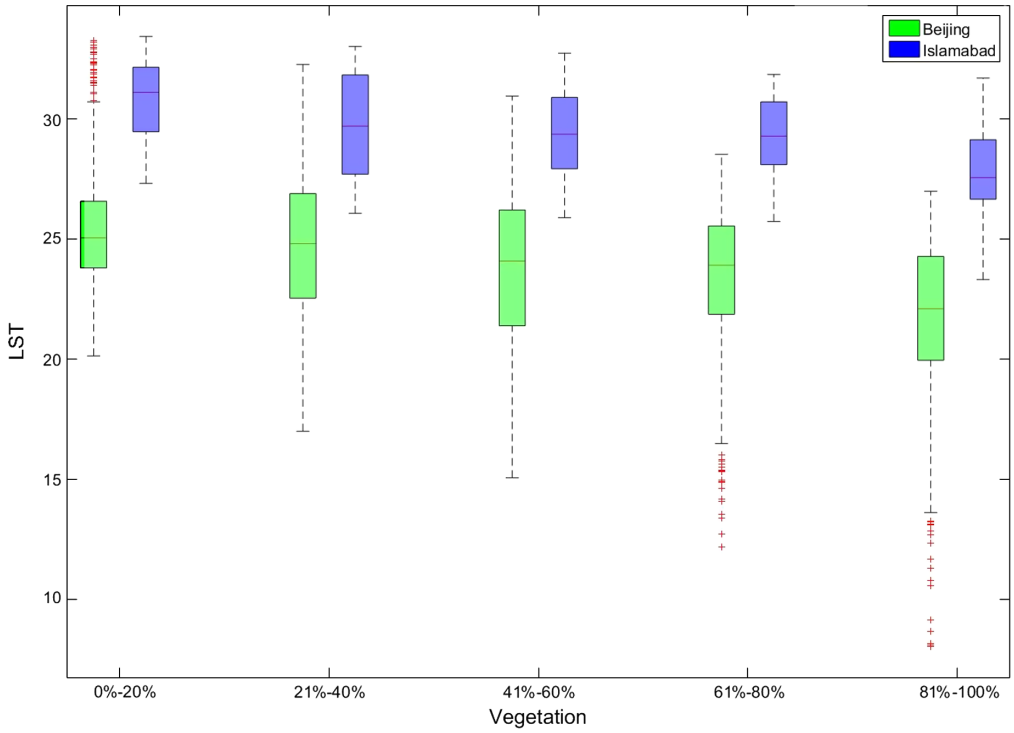

Fig. 7 Boxplot of LST for the rural area based on vegetation area quantiles.

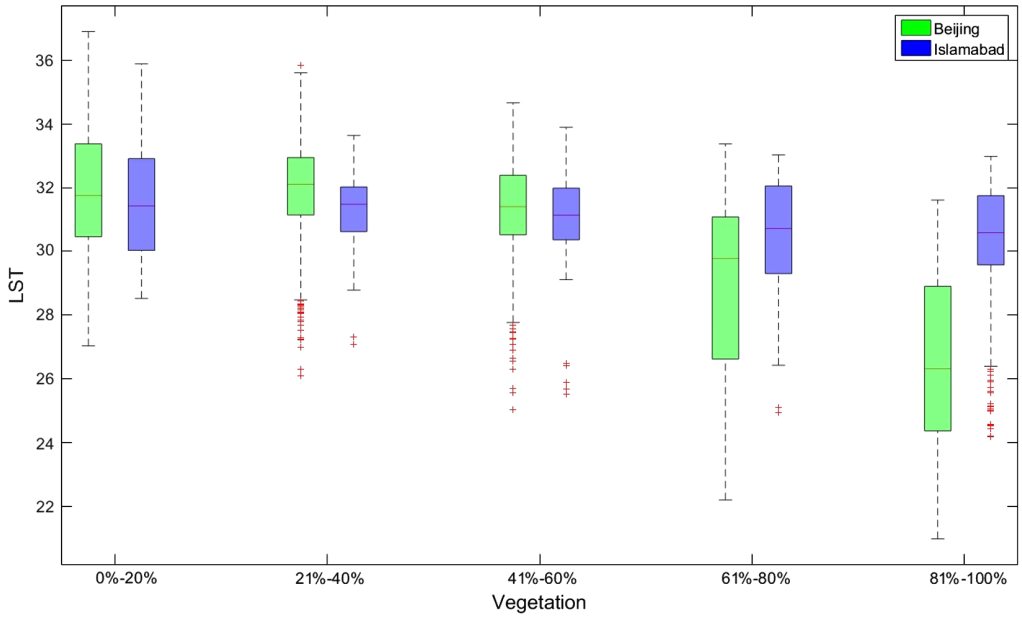

Fig. 8 Boxplot of LST for the urban area based on vegetation area quantiles.

maximum temperature in that region is 33°C. On the other hand, surface temperature does not change more rapidly in Islamabad, and there is a short surface temperature range from 23°C to 33°C, but the mean surface temperature of Islamabad is higher than Beijing in rural regions.

It is clear from Fig. 9 that the same trend as the rural region was observed in suburban regions. Again, in this region, a higher mean surface temperature is observed in Islamabad than that in Beijing. From Fig. 9, it is clear that the mean temperature is decreasing within quantiles of 1 km^2 with the increase in vegetation proportion in both cities.

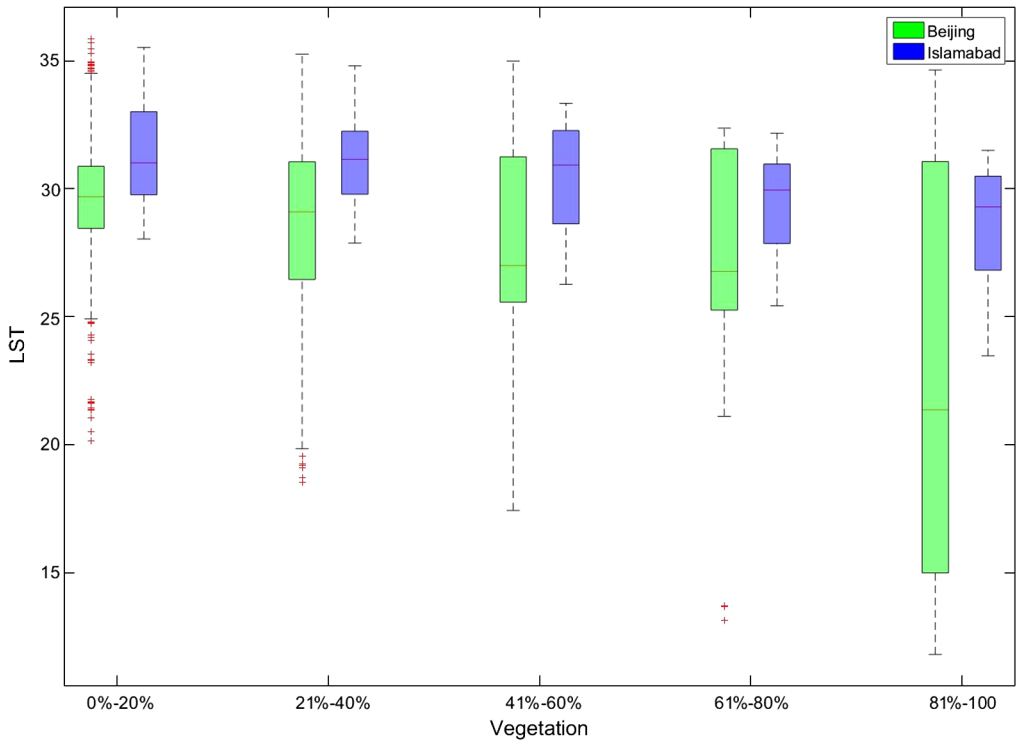

Fig. 9 Boxplot of LST for the suburban area based on vegetation area quantiles.

Islamabad's temperature varies from 24°C to 35.5°C, while Beijing's surface temperature varies more rapidly between the range of 12°C and 36°C. However, the average temperature of Beijing is less than Islamabad in all intervals of vegetation fractions of the suburban region.

The results of urban regions are very interesting and different from the previous trend of rural and suburban regions. Based on vegetation fraction intervals, the average surface temperature of Islamabad ranges from 30°C to 31.5°C, while Beijing ranges between 26°C and 32.5°C. Islamabad has a greater fraction of vegetation per unit area (Table 5) and scattered population in the urban zone as compared to Beijing. On the other hand, Beijing is a more populated and industrialized city. The built-up area of Beijing is more than 10 times greater than that of Islamabad. There is more built-up area and less urban vegetation in Beijing than in Islamabad, which could be one of the main reasons for the observed higher LST in the urban zone of Beijing. The mean surface temperature of Beijing is 1°C higher than Islamabad in the core city areas, as shown in Fig. 8.

3.2 *Relationship Between LST and Built-Up Areas*

Figure 10 shows the overall pattern of LST in the urban area for the study sites. It can be seen in Fig. 10, for Beijing, that higher values of surface temperature start after the 40% proportion of built-up area within the defined quantiles in comparison to Islamabad.

Therefore, above a 40% proportion of the built-up area within 1 km^2, Beijing has a higher surface temperature than Islamabad. The average temperature of Beijing above the 40% proportion is 31°C, while that of Islamabad is around 30°C. Conversely, Islamabad has higher values of LST under the 40% proportion of the built-up area within 1 km^2, i.e., for Islamabad, it is around 28.5°C, and for Beijing, it is about 26°C. Therefore, more than a 40% fraction of built-up area means that most of the quantiles belong to the core city area because in the rural and suburban regions, the population is not dense, and so, the urban area intensity is also very low. Therefore, it also verifies the results of the vegetation fraction with the surface temperature that the core city area of Beijing is hotter than Islamabad, as was expected.

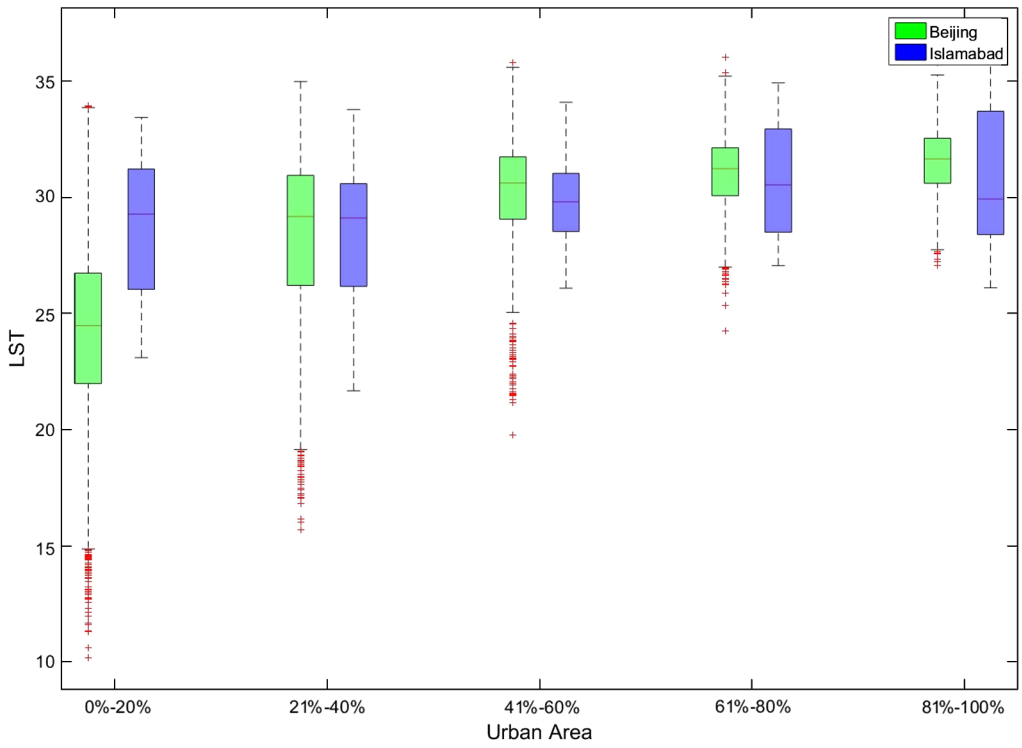

Fig. 10 Boxplot of LST based on the built-up area quantiles.

3.3 *Ecological Evaluation of Temperature and the Quality of Living in Beijing and Islamabad*

The urban thermal field variance index (UTFVI) was applied to evaluate the urban surface temperature quantitatively. It can be calculated as

$$\mathrm{UTFVI} = \frac{T_s}{T_s - T_{\mathrm{mean}}}, \tag{8}$$

where T_s represents the surface temperature of a certain point, and T_{mean} is the mean value of the surface temperature of the study sites.

To demonstrate the changes of surface temperature quantitatively, it was further divided into six categorical ecological evaluation indices.[58,59] Table 8 presents the definite thresholds of UTFVI levels. Figure 11 shows the classification of the ecological evaluation index.

As far as the terrain of Islamabad and Beijing is concerned, both cities vary from plain to hilly and hilly to mountainous, with Beijing having slightly steeper slopes. Most of the hilly and mountainous lands are undeveloped and covered with natural reserves and country parks. These undeveloped areas are rich in green and healthy vegetation with scattered or no population (Fig. 12), having an excellent ecoenvironment evaluation index. However, the increasing trends of vegetation degradation are giving space to urban and industrial developments, so making cities warmer and supporting the UHI phenomenon. The continuous increase in population

Table 8 Threshold of the UTFVI for ecological evaluation.

UTFVI	UHI phenomena	Ecological evaluation index
<0.000	None	Excellent
0.000 to 0.005	Weak	Good
0.005 to 0.010	Middle normal	Normal
0.010 to 0.015	Strong	Bad
0.015 to 0.020	Stronger	Worse
>0.020	Strongest	Worst

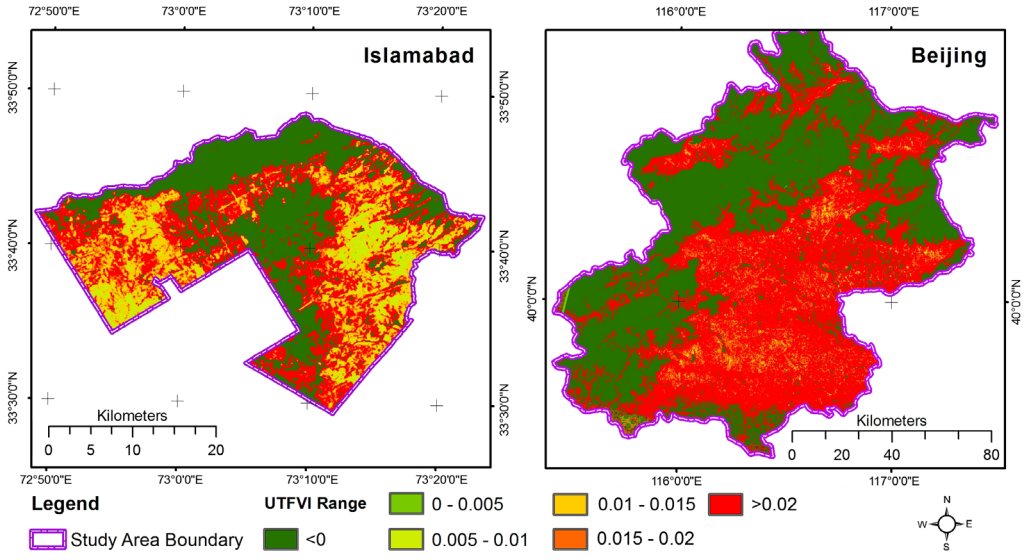

Fig. 11 UTFVI classification map for the ecological evaluation in Beijing and Islamabad.

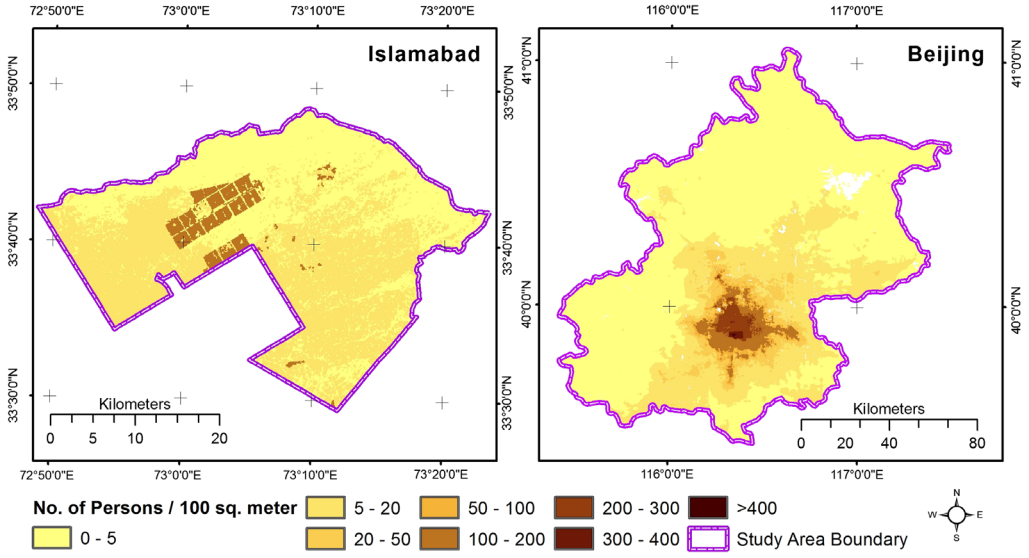

Fig. 12 Spatial distribution of the population in Beijing and Islamabad.

Table 9 Quality of living based on the ecological evaluation index.

UHI phenomena	Ecological evaluation index	Beijing population (%)	Islamabad population (%)
None	Excellent	6.76	23.74
Weak	Good	0.16	0.01
Middle normal	Normal	0.01	3.89
Strong	Bad	1.82	10.71
I stronger	Worse	16.24	11.75
Strongest	Worst	75.01	49.90

is leading to a poor ecoenvironment and strengthening the UHI phenomenon. As a result, the quality of living is decreasing from bad to worse 12.

The classification map shows that the Beijing urban area is more severally affected as compared to Islamabad. Table 9 shows that two extreme levels of ecological evaluation claimed areas of both cities: the excellent ecoenvironment at UTFVI < 0 and the worst when UTFVI > 0.020.

4 Discussion

The study was conducted to evaluate the environmental conditions based on EO-supported ecoenvironmental indices in Beijing, China, and a poorly studied Islamabad, Pakistan. There are substantial LST fluctuations among all three regions of urban, suburban, and rural (LCZ) of Beijing and Islamabad. Descriptive statistical and image processing methods were applied to investigate the variations in temperatures of both cities by testing both land covers. As expected, LST decreasing trends from urban to rural areas were found. A strong relationship was observed between vegetation fraction and LST for each region in each grid cell. The first finding of this study is Beijing's high LST in urban regions compared to Islamabad. The mean air temperature of both Beijing and Islamabad remains less than the surface temperature throughout the year, as shown in Figs. 13 and 14. Therefore, surface temperature extracted from the MODIS product was drawn against mean air temperature for all seasons, which indicates that the surface temperature for all of the regions is greater than the air temperature.

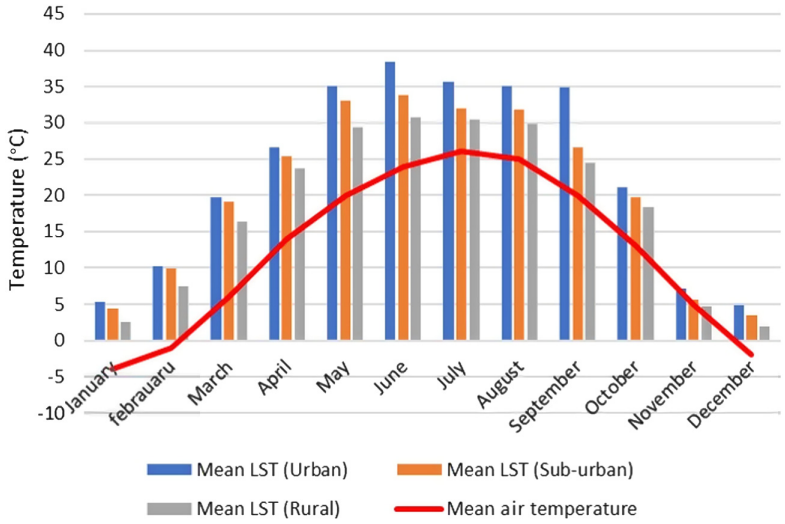

Fig. 13 MODIS product-based surface temperature variations with air temperature for Beijing.

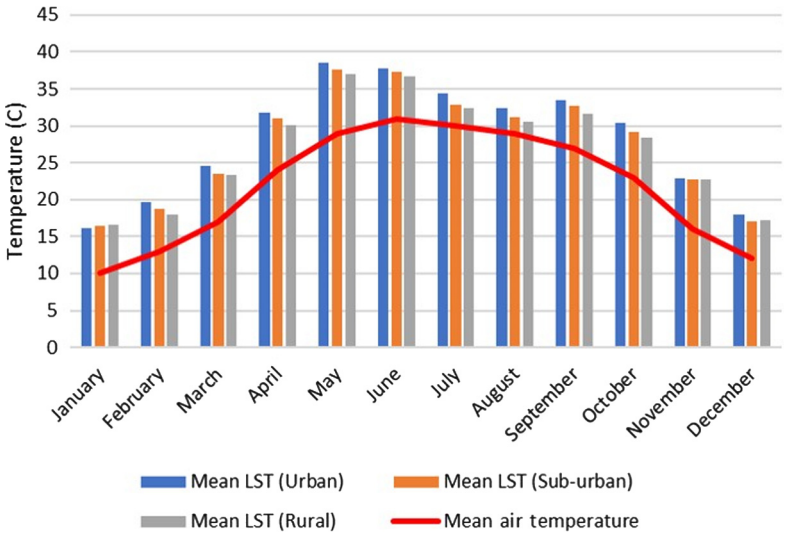

Fig. 14 MODIS product-based surface temperature variations with air temperature for Islamabad.

Here, one thing is notable: the air temperature of Islamabad is greater, but the surface temperature is lower than Beijing in urban regions of the cities, which shows the higher effect of UHI in Beijing than Islamabad. Normally, the difference in air temperature is mainly due to the difference in elevation and latitudes, as shown in Figs. 13 and 14.

Beijing is situated at higher latitudes than Islamabad, and elevation differences also exist there, especially in rural areas of both cities; therefore, the average air temperature of Islamabad remains greater than Beijing throughout the year, as shown in the figures. In rural and suburban areas, the fraction of vegetation is very high, and the population density is very low, so there is a much less probability of anthropogenic activities; therefore, the air temperature trend is continuous. On the other hand, Beijing's population is more than 10 times that of Islamabad, hence the urban area expansion, and so, the opposite trend was observed in urban areas. The average LST of the urban region of Beijing was computed as 31°C, while that of Islamabad is about 30°C. Furthermore, the maximum LST of Beijing in August and September was calculated as 37°C, whereas Islamabad's temperature is around 35.5°C. This clarifies how vegetation and urban expansion play a role in changing the surface temperature. Therefore, the large proportion of vegetation and the low rate of urban land expansion and industrialization are helping Islamabad to keep surface heat under control, as compared to Beijing.

Table 10 Linear correlation of NDVI and NDBI with LST [coefficient of determination (R^2)].

	NDVI-LST			NDBI-LST		
Site name	Urban	Suburban	Rural	Urban	Suburban	Rural
Beijing	0.511	0.379	0.294	0.255	0.388	0.631
Islamabad	0.737	0.434	0.323	0.427	0.491	0.597

The same procedure was applied on built-up areas and found that the higher proportion of built-up area within a grid cell of 1 km^2 corresponds to considerably higher LST, while a higher vegetation fraction within a defined grid cell resulted in a significant decrease in LST. The built-up area of Beijing has higher LST values above the 40% proportion of built-up area within 1 km^2, while below 40%, Islamabad's LST is on the higher side. The trend, high built-up fraction higher LST and high vegetation fraction lower LST, is similar to the conclusions of Alavipanah et al.[15]

The linear correlation of NDVI and NDBI with LST also indicates a higher evapotranspiration in rural regions and minimum in the urban regions. NDBI shows a positive linear correlation with LST and maximum in urban regions of Beijing and Islamabad. It is shown in Table 10. The relationship of LST with NDVI has already been documented extensively in previous studies. The NDVI is being considered as a vegetation coverage characteristic to analyze the thermal environments of urban regions in previous researches and our results coincide with a number of researches.[8,12]

Although the UHI intensity is basically controlled by evapotranspiration differences between urban and urban regions, UHI patterns also depend on the geographic environment of different cities.[60] Therefore, due to different geographic locations of Beijing and Islamabad, the growth condition of different vegetation types may impact the UHI distribution in cities.[61] Another factor is human activity. It is a very important factor in explaining the vegetation changes, because socioeconomic impacts on vegetation cover are spatially heterogeneous for different geographical and environmental regions.[62] The low population density of Islamabad means less probability of anthropogenic activities, especially in urban zones. Therefore, fewer human activities can also be one of the reasons of better environmental conditions of Islamabad than that of Beijing in urban zones. The rural regions of Beijing have some wetlands that can affect the evapotranspiration rate for nearby areas. Therefore, these factors can make a significant difference in the consistency of LST in different geographically located vegetated areas.

Beijing is composed of 11 districts, and Islamabad is divided into five administrative zones (no specific names exist for the Islamabad zones). By plotting vegetation area against population density in administrative units, the most populated zones/districts are less vegetated as expected, as shown in Figs. 15 and 16. The results of Beijing indicate that ~83% of the total population is living in the urban zone, 11% in suburban, and only 6% in the rural zone. Therefore, the urban area, especially Beijing Shi (the core city area), is very congested, where the population density is around 9534/km^2, while the urban zone defined for this study has a population density of around 5354/km^2. The population density of suburban and rural regions was calculated as 543 and 141 persons/km^2, respectively. In the case of Islamabad, 85% of the total population is living in urban, 11% in suburban, and 4% in rural regions, whereas the population densities are 2736, 597, and 112 persons/km^2 for urban, suburban, and rural regions, respectively. Zone-1 is the most populated zone with a low fraction of vegetation compared to other zones, and it has a population density of 4542 persons/km^2. The results of Figs. 15 and 16 indicate that Islamabad has a higher vegetation fraction and less population density per unit area as compared to Beijing. The rapid urbanization in Beijing has increased the UHI effects. The UHI effect in Beijing suddenly started intensifying in 1988, and within the last few years, it has become a very hot issue.[63] The UHI of Beijing spatially has lower LST in the north direction and a higher LST in the south direction, which is represented as the NE-SW axis.[64] This is because of the greater urbanization in the south direction, hence the increase in impervious surfaces, which are directly correlated with LST.[65] Beijing remains under a high UHI effect throughout the year, except the winter

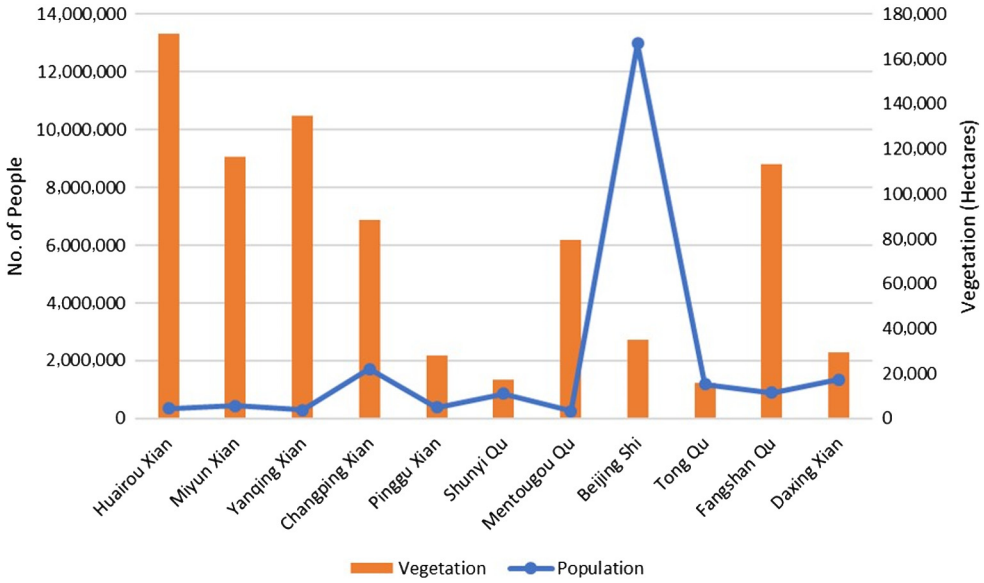

Fig. 15 Population distribution and vegetation cover analysis in the administrative units of Beijing.

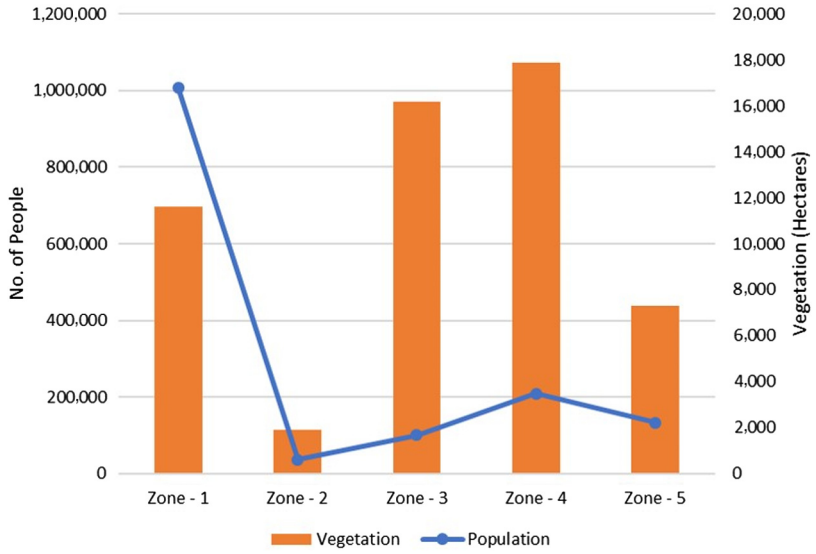

Fig. 16 Population distribution and vegetation cover analysis in the administrative units of Islamabad.

season.[66] The increase in vegetation cover proves beneficial to mitigate the UHI effect in urban regions in the summer season and keeps the surface warmer in the winter season.[67] On the other hand, till now, there have been no studies on the UHI of Islamabad. The comparison has been made between Rawalpindi and Islamabad on the local level, but it is not a published research. Islamabad should learn from Beijing to take the initiatives such as "wedge green belt" before facing the same UHI issues such as Beijing. China government has already taken the "wedge green belt" initiative in order to increase the tree cover canopy of Beijing.[64,68]

Figures 15 and 16 show the proportion of vegetation per km^2 of Islamabad is higher than Beijing. The vegetation degradation and urban sprawl are two of the most influential factors for increasing the surface temperature of the core city area of Beijing. This increase in surface temperature affects the overall urban thermal environment, increases the intensity of UHI, destroys the ecoenvironment, and ultimately lowers the quality of living. Therefore, vegetation is one of the key parameters that can contribute effectively to control surface heat islands.[11]

This study will also help in understanding the importance of EO-supported environmental indices for ecological evaluation. UTFVI has already been used in some researches[58,59] but has rarely been used an indicator of quality of living to indicate the inhabitants under poor, normal, and good ecoenvironmental conditions. The results of UTFVI indicate that 91% of the population of Beijing is living under intense UHI, and 7% is living under good conditions, while less than 2% is living under normal UHI intensity. On the other hand, the ecoenvironment conditions of Islamabad are comparatively better than Beijing. In Islamabad, 61% of the population is living under intense UHI, 15% population is under normal, while 24% is living in a good condition of the ecoenvironment, as shown in Table 9. The combination of EO-supported parameters and the UTFVI classification was found to be very effective for studying the quality of living in the context of the UHI phenomenon. Furthermore, the classified map of the ecological evaluation of Islamabad and Beijing can provide meaningful information for policy makers, urban environment planners, and managers to analyze the ecoenvironmental quality for future urban planning. More studies are recommended by combining EO data with thermal classification indices such as UTFVI, especially in Islamabad. This study can also be further advanced by synchronizing the socioeconomic parameter with this combination of UTFVI and EO-supported datasets. There are some limitations of this study; as both cities are very different in geographical location, population, area covered, climate, and socioeconomic activities, it was very difficult to define a scale for the comparison of the vegetation for these two cities. The field reference data were not available, so this study relies on EO products using image-processing techniques. There are some suggestions from the previous studies on Beijing; for example, Chen et al. suggested balanced development with as many green spaces as possible;[69] Zhi et al. also suggested the increase in greening measure with the investigation of the effect of human activities on the thermal environments of urban regions;[64] and Liu et al. suggested that planting with an equal distribution can mitigate UHI intensity.[70]

5 Conclusions

The satellite remote sensing data-based LCZ provided the basis to compare the cooling effect of vegetation to study the ecoenvironmental condition of two cities. The high spatial resolution EO-supported datasets proved to be very effective for studying urban thermal environments, ecoenvironmental conditions, and indicators for the quality of living in rapidly growing cities. The study highlights that vegetation fractions and surface temperature have a negative relationship, whereas a positive relationship was observed between built-up area fractions and surface temperature. Although vegetation is not the only factor to control the UHI phenomenon, optimum green spaces can play an anchoring role in cooling down the temperature of the impervious surfaces of the urban periphery. Furthermore, the higher intensity of urbanization and fewer green spaces are some of the reasons for the higher surface temperature in the urban zone of Beijing compared to the same zone of Islamabad. The results of the ecological evaluation index indicated the highest UHI phenomenon in core city areas and the minimum in mountainous or vegetated areas. Therefore, the intense urbanization is destroying the ecoenvironments of cities and affecting the quality of living very badly. More than 90% of the population of Beijing is living under intense UHI, and less than 7% is living in good conditions. Islamabad's condition is comparatively better, where around 62% of the population is under intense UHI, while 24% of the total population is living in good conditions. Islamabad needs to learn from Beijing's current situation, and urban planners and environmentalists should focus on proper urban planning and reasonable city layouts in the future. Different studies on the thermal properties of UHI and the distribution of vegetation not only enhance our understandings about urban ecology and moderating urban outdoor thermal comfort with urban ecosystem services, but they also assist with reducing power consumption required for cooling the cities, the emission of carbon dioxide CO_2 and pollution with proper adaptation to global and regional climate change. As a result, further studies are required, by combining satellite imagery with ground referenced data, to determine the local- and regional-scale impacts of the green infrastructure of urban areas. Furthermore, these rapidly urbanizing landscapes can be investigated on the basis of different climate change scenarios to contribute to the efforts of mitigating the impact of carbon dioxide emissions.

UHI can be mitigated by increasing the amount of green spaces in the form of greening roofs, by constructing parks within the main city area and by planting trees along roads and in vacant areas. Islamabad, being at the early growth stage, should learn from the current situation of Beijing for urban planning in the future.

Acknowledgments

Special Fund for Forest Scientific Research in the Public Welfare (No. 201504323) are acknowledged for their financial support. The authors are very grateful to the Institute of Remote Sensing and Digital Earth (RADI), the University Chinese Academy of Sciences (UCAS) Beijing, for providing the high-resolution imagery of the Gaofen-1 satellite. The authors declare no conflict of interest. Two authors, Shahid Naeem and Bipin Kumar Acharya, acknowledge the Chinese Academy of Sciences (CAS) and The World Academy of Sciences (TWAS) for awarding the CAS-TWAS President's Fellowship to carry out the research.

References

1. E. F. Lambin and H. J. Geist, *Land-Use and Land-Cover Change: Local Processes and Global impacts*, Springer Science & Business Media, New York (2008).
2. H. Sajjad and M. Iqbal, "Impact of urbanization on land use/land cover of Dudhganga watershed of Kashmir Valley, India," *Int. J. Urban Sci.* **16**(3), 321–339 (2012).
3. M. Mohan et al., "Dynamics of urbanization and its impact on land-use/land-cover: a case study of megacity Delhi," *J. Environ. Prot.* **2**(09), 1274–1283 (2011).
4. Y. Wu, X. Zhang, and L. Shen, "The impact of urbanization policy on land use change: a scenario analysis," *Cities* **28**(2), 147–159 (2011).
5. T. R. Oke, "The energetic basis of the urban heat island," *Q. J. R. Meteorol. Soc.* **108**(455), 1–24 (1982).
6. J. B. Basara et al., "The impact of the urban heat island during an intense heat wave in Oklahoma City," *Adv. Meteorol.* **2010**, 230365 (2010).
7. W. Kuang et al., "A comparative analysis of megacity expansions in China and the US: patterns, rates and driving forces," *Landscape Urban Plann.* **132**, 121–135 (2014).
8. L. M. Gartland, *Heat Islands: Understanding and Mitigating Heat in Urban Areas*, pp. 1–200, Routledge, London, United Kingdom (2012).
9. Q. Weng, D. Lu, and J. Schubring, "Estimation of land surface temperature–vegetation abundance relationship for urban heat island studies," *Remote Sens. Environ.* **89**(4), 467–483 (2004).
10. Q. Weng, "Thermal infrared remote sensing for urban climate and environmental studies: methods, applications, and trends," *ISPRS J. Photogramm. Remote Sens.* **64**(4), 335–344 (2009).
11. J. Cristóbal, M. Ninyerola, and X. Pons, "Modeling air temperature through a combination of remote sensing and GIS data," *J. Geophys. Res.: Atmos.* **113**(D13), 1–13 (2008).
12. R. Amiri et al., "Spatial–temporal dynamics of land surface temperature in relation to fractional vegetation cover and land use/cover in the Tabriz urban area, Iran," *Remote Sens. Environ.* **113**(12), 2606–2617 (2009).
13. Q. Le-Xiang, C. Hai-Shan, and J. Chang, "Impacts of land use and cover change on land surface temperature in the Zhujiang delta11project supported by the science and technology project foundation of Guangzhou (no. 2005z3-d0551) and the science and technology project foundation of Guangzhou education bureau (no. 62026)," *Pedosphere* **16**(6), 681–689 (2006).
14. H. Ding and W. Shi, "Land-use/land-cover change and its influence on surface temperature: a case study in Beijing city," *Int. J. Remote Sens.* **34**(15), 5503–5517 (2013).
15. S. Alavipanah et al., "The role of vegetation in mitigating urban land surface temperatures: a case study of Munich, Germany during the warm season," *Sustainability* **7**(4), 4689–4706 (2015).
16. I. Ogashawara and V. D. S. B. Bastos, "A quantitative approach for analyzing the relationship between urban heat islands and land cover," *Remote Sens.* **4**(11), 3596–3618 (2012).

17. Y. Xiong et al., "The impacts of rapid urbanization on the thermal environment: a remote sensing study of Guangzhou, South China," *Remote Sens.* **4**(7), 2033–2056 (2012).
18. W. Kuang et al., "What are hot and what are not in an urban landscape: quantifying and explaining the land surface temperature pattern in Beijing, China," *Landscape Ecol.* **30**(2), 357–373 (2015).
19. J. Li et al., "Impacts of landscape structure on surface urban heat islands: a case study of Shanghai, China," *Remote Sens. Environ.* **115**(12), 3249–3263 (2011).
20. J. Zhou, B. Yu, and J. Qin, "Multi-level spatial analysis for change detection of urban vegetation at individual tree scale," *Remote Sens.* **6**(9), 9086–9103 (2014).
21. B. Ahmed et al., "Simulating land cover changes and their impacts on land surface temperature in Dhaka, Bangladesh," *Remote Sens.* **5**(11), 5969–5998 (2013).
22. Y. Jiang, P. Fu, and Q. Weng, "Assessing the impacts of urbanization-associated land use/cover change on land surface temperature and surface moisture: a case study in the Midwestern United States," *Remote Sens.* **7**(4), 4880–4898 (2015).
23. C. Du et al., "Split-window algorithm for estimating land surface temperature from Landsat 8 TIRS data," in *IEEE Int. Geoscience and Remote Sensing Symp. (IGARSS '14)*, pp. 3578–3581, IEEE (2014).
24. T. Honjo and T. Takakura, "Analysis of temperature distribution of urban green spaces using remote sensing data," *J. Jpn. Inst. Landscape Archit.* **49**, 299–304 (1986).
25. M. Richter and U. Weiland, *Applied Urban Ecology: A Global Framework*, Wiley-Blackwell, Hoboken, New Jersey (2011).
26. "Beijing Municipal Bureau of Statistics (BMBS)," *Beijing Statistical Yearbook*, China State Statistical Press, Beijing, China (2010), in Chinese.
27. X. Xia et al., "Variation of column-integrated aerosol properties in a Chinese urban region," *J. Geophys. Res.: Atmos.* **111**(D5), 1–10 (2006).
28. J. Zhang et al., "The diurnal and seasonal characteristics of urban heat island variation in Beijing city and surrounding areas and impact factors based on remote sensing satellite data," *Sci. China Ser. D-Earth Sci.* **48**(Suppl.), 220–220 (2005).
29. Q. Ge et al., "The effect of climate change on the fall foliage vacation in China," *Tourism Manage.* **38**, 80–84 (2013).
30. Z. Qiao, G. Tian, and L. Xiao, "Diurnal and seasonal impacts of urbanization on the urban thermal environment: a case study of Beijing using MODIS data," *ISPRS J. Photogramm. Remote Sens.* **85**, 93–101 (2013).
31. G. R. Memon, "Education in Pakistan: the key issues, problems and the new challenges," *J. Manage. Soc. Sci.* **3**(1), 47–55 (2007).
32. M. H. Shah and N. Shaheen, "Seasonal behaviours in elemental composition of atmospheric aerosols collected in Islamabad, Pakistan," *Atmos. Res.* **95**(2), 210–223 (2010).
33. C. T. Lloyd et al., "High resolution global gridded data for use in population studies," *Sci. Data* **4**(170001) (2017).
34. F. R. Stevens et al., "Disaggregating census data for population mapping using random forests with remotely-sensed and ancillary data," *PLoS One* **10**(2), e0107042 (2015).
35. V. A. Alegana et al., "Fine resolution mapping of population age-structures for health and development applications," *J. R. Soc. Interface* **12**(105), 20150073 (2015).
36. P. Deville et al., "Dynamic population mapping using mobile phone data," *Proc. Natl. Acad. Sci. U. S. A.* **111**(45), 15888–15893 (2014).
37. A. Tatem, D. Weiss, and C. Pezzulo, *Pilot High Resolution Poverty Maps*, University of Oxford, Southampton (2013).
38. M. Jin et al., "A practical split-window algorithm for retrieving land surface temperature from Landsat-8 data and a case study of an urban area in China," *Remote Sens.* **7**(4), 4371–4390 (2015).
39. Z.-L. Li et al., "Satellite-derived land surface temperature: current status and perspectives," *Remote Sens. Environ.* **131**, 14–37 (2013).
40. O. Rozenstein et al., "Derivation of land surface temperature for Landsat-8 TIRS using a split window algorithm," *Sensors* **14**(4), 5768–5780 (2014).
41. J. C. Jiménez-Muñoz et al., "Land surface temperature retrieval methods from Landsat-8 thermal infrared sensor data," *IEEE Geosci. Remote Sens. Lett.* **11**(10), 1840–1843 (2014).

42. F. Wang et al., "An improved mono-window algorithm for land surface temperature retrieval from Landsat 8 thermal infrared sensor data," *Remote Sens.* **7**(4), 4268–4289 (2015).
43. Z. Qin, A. Karnieli, and P. Berliner, "A mono-window algorithm for retrieving land surface temperature from Landsat TM data and its application to the Israel-Egypt border region," *Int. J. Remote Sens.* **22**(18), 3719–3746 (2001).
44. D. Skoković et al., "Calibration and validation of land surface temperature for landsat8-tirs sensor," in *LPVE (Land Product Validation and Evolution*, ESA/ESRIN, Frascati (Italy) (2014).
45. M. Baatz, "Multiresolution segmentation: an optimization approach for high quality multi-scale image segmentation," in *Angewandte Geographische Informations-Verarbeitung XII*, J. Strobl, T. Blaschke, and G. Griesbner, Eds., pp. 12–23, Wichmann Verlag, Karlsruhe, Germany (2000).
46. S. Lang and D. Tiede, *Definiens Developer, GIS Business 9/2007*, pp. 34–37, ABC Verlag, Munich, Germany (2007).
47. M. Neubert, H. Herold, and G. Meinel, "Assessing image segmentation quality–concepts, methods and application," in *Object-Based Image Analysis*, pp. 769–784, Springer, Berlin, Heidelberg (2008).
48. G. J. Hay et al., "An automated object-based approach for the multiscale image segmentation of forest scenes," *Int. J. Appl. Earth Obs. Geoinf.* **7**(4), 339–359 (2005).
49. W. Siler and J. J. Buckley, *Fuzzy Expert Systems and Fuzzy Reasoning*, John Wiley & Sons, Hoboken, New Jersey (2005).
50. J. A. Richards and J. Richards, *Remote Sensing Digital Image Analysis*, Vol. **3**, Springer, Berlin, Heidelberg (1999).
51. I. D. Stewart and T. R. Oke, "Local climate zones for urban temperature studies," *Bull. Am. Meteorol. Soc.* **93**(12), 1879–1900 (2012).
52. Z. Yang et al., "Accuracy assessment and inter-comparison of eight medium resolution forest products on the loess plateau, China," *ISPRS Int. J. Geo-Inf.* **6**(5), 152 (2017).
53. A. Tilahun and B. Teferie, "Accuracy assessment of land use land cover classification using Google earth," *Am. J. Environ. Prot.* **4**, 193–198 (2015).
54. A. Ghosh and P.K. Joshi, "A comparison of selected classification algorithms for mapping-bamboo patches in lower Gangetic plains using very high resolution WorldView 2 imagery," *Int. J. Appl. Earth Obs. Geoinf.* **26**, 298–311 (2014)
55. S. Yadav, I. Rizvi, and S. Kadam, "Comparative study of object based image analysis on high resolution satellite images for urban development," *Int. J. Tech. Res. Appl.* **31**, 105–110 (2015)
56. Q. Feng, J. Liu, and J. Gong, "UAV remote sensing for urban vegetation mapping using random forest and texture analysis," *Remote Sens.* **7**(1), 1074–1094 (2015).
57. Z. Kaszta, "Seasonal separation of African savanna components using worldview-2 imagery: a comparison of pixel-and object-based approaches and selected classification algorithms," *Remote Sens.* **8**(9), 763 (2016)
58. R. Alfraihat, G. Mulugeta, and T. Gala, "Ecological evaluation of urban heat island in Chicago City, USA," *J. Atmos. Pollut.* **4**(1), 23–29 (2016).
59. L. Liu and Y. Zhang, "Urban heat island analysis using the Landsat TM data and ASTER data: a case study in Hong Kong," *Remote Sens.* **3**(7), 1535–1552 (2011).
60. Y.-Y. Choi, M.-S. Suh, and K.-H. Park, "Assessment of surface urban heat islands over three megacities in east Asia using land surface temperature data retrieved from COMS," *Remote Sens.* **6**(6), 5852–5867 (2014).
61. J. Tsou et al., "Urban heat island assessment using the Landsat 8 data: a case study in Shenzhen and Hong Kong," *Urban Sci.* **1**(1), 10 (2017).
62. M. Jiang et al., "Human activity influences on vegetation cover changes in Beijing, China, from 2000 to 2015," *Remote Sens.* **9**(3), 271 (2017).
63. M. Wang et al., "Research on urban heat island effect during Beijing urbanization process by remote sensing and its impact on environmental health," in *IEEE Int. Geoscience and Remote Sensing Symp. (IGARSS '12)*, pp. 507–510, IEEE (2012).
64. Z. Qiao et al., "Influences of urban expansion on urban heat island in Beijing during 1989–2010," *Adv. Meteorol.* **2014**, 187169 (2014).

65. R.-B. Xiao et al., "Spatial pattern of impervious surfaces and their impacts on land surface temperature in Beijing, China," *J. Environ. Sci.* **19**(2), 250–256 (2007).
66. G. Cai, M. Du, and Y. Xue, "Monitoring of urban heat island effect in Beijing combining ASTER and tm data," *Int. J. Remote Sens.* **32**(5), 1213–1232 (2011).
67. X. Zhao et al., "Analyzing the relationship between urban heat island and land use/cover changes in Beijing using remote sensing images," *Proc. SPIE* **7454**, 74541J (2009).
68. "13th Five-Year," Planning and Development of Major Infrastructure in Beijing, http://zhengwu.beijing.gov.cn/gh/dt/t1449303.htm (07 March 2017).
69. W. Chen et al., "The investigation of urbanization and urban heat island in Beijing based on remote sensing," *Procedia–Soc. Behav. Sci.* **216**, 141–150 (2016).
70. K. Liu et al., "Quantifying spatial–temporal pattern of urban heat island in Beijing: an improved assessment using land surface temperature (LST) time series observations from LANDSAT, MODIS, and Chinese new satellite GaoFen-1," *IEEE J. Sel. Top. Appl. Earth Obs. Remote Sens.* **9**(5), 2028–2042 (2016).

Shahid Naeem received his master's degree in space sciences from the University of the Punjab, Pakistan, in 2009. Currently, he is a PhD scholar at Division of Environmental Health, State Key Laboratory, Institute of Remote Sensing and Digital Earth (RADI), Chinese Academy of Science, Beijing, China. His research interests include applications of remote sensing in urban ecosystems.

ChunXiang Cao is a professor, director of the Department of Environment Health Remote Sensing, State Key Lab of Resources and Environmental Information System (LREIS), RADI, Chinese Academy of Sciences (CAS). His research field is the diagnosis of environmental health by remote sensing, mainly including forest remote sensing, quantitative remote sensing inversion of ecological environmental parameters, and public health research using spatial information technology.

Mirza Muhammad Waqar received his master's degree in remote sensing and geographic information science from the National University of Sciences and Technology, Pakistan, in 2012. He is currently a PhD scholar at Josaphat Microwave Remote Sensing Laboratory, Center for Environmental Remote Sensing, Chiba University, Japan. His current research interests include forest biophysical parameters estimation using Pol-InSAR.

Chen Wei is an assistant professor at RADI, CAS. He got his PhD in Kyoto University in 2014. Now his research focuses on diagnosis of forest health by remote sensing, quantitative remote sensing inversion of ecological parameters as well as wetland health research using spatial information technology. He has published more than 45 papers and serves as first author in 21 of them. He is undertaking several projects and has published three monographs.

Bipin Kumar Acharya received his MPhil degree in geography from the University of Bergen, Norway, in 2012. Currently, he is a PhD scholar at the State Key Laboratory of Environmental Health, RADI, CAS. His research interests include applications of remote sensing in environmental health diagnosis.